Optimal Planning of Storage in Power Systems Integrated With Wind Power Generation

Peng Xiong and Chanan Singh, *Fellow, IEEE*

***Abstract*—This paper proposes an approach for determining the optimal location and size of an energy storage system (ESS) in a power system network integrated with uncertain wind power generation. The uncertainty of wind power output is represented by a scenario tree model, so that the nonanticipative behavior of operating decisions under system uncertainties can be properly addressed. The proposed formulation is too huge to be solved directly, so a Benders decomposition algorithm is applied to reduce the computational burden. Case studies are conducted to illustrate the influence of ESS on power system operation. It is shown that increasing the capital investment on ESS can reduce the daily operating cost of the power system. A capital/operating cost frontier is presented in this paper to demonstrate the tradeoff between ESS capital investment and daily operating cost, and to show how ESS planning decisions are affected by the budget for investment.**

***Index Terms*—Decomposition algorithm, energy storage system (ESS), expansion planning, wind power generation.**

NOMENCLATURE

Indices

d	Indices of operating days.
l	Indices of transmission lines.
m	Indices of buses.
n	Indices of generators.
s	Indices of wind power scenarios.
t	Indices of time steps.
w	Index of bus integrated with wind power generation.

Sets

$\mathcal{D}$	Set of all days considered.
$\mathcal{L}$	Set of all transmission lines.
$\mathcal{M}$	Set of all buses.
$\mathcal{N}$	Set of all generators.
$\mathcal{N}_m$	Set of all generators connected to bus m.
$\mathcal{S}$	Set of all wind power scenarios.
$\mathcal{T}$	Set of all time steps in one day.

System Parameters

D_{mtd}	Electricity demand at bus m during time step t in day d (MW).
$F_l^{\max}$	Maximum capacity of transmission line l (MW).
$G_n^{\max}$	Maximum power generation of conventional unit n (MW).
$G_n^{\min}$	Minimum power generation of conventional unit n (MW).
K_{ml}	Distribution factor of transmission line l due to the net power injection at bus m.
$H_m^{\max}$	Maximum energy rating limitation of storage system at bus m (MWh).
$H_m^{\min}$	Minimum energy rating limitation of storage system at bus m (MWh).
NS	Lifespan of storage units (years).
$R_m^{\max}$	Maximum power rating limitation of storage system at bus m (MW).
$R_m^{\min}$	Minimum power rating limitation of storage system at bus m (MW).
R_n^R	Ramp-rate limitation of conventional generator n (MW/h).
α_m^C	Charging efficiency of energy storage system (ESS) located at bus m.
α_m^D	Discharging efficiency of ESS located at bus m.
Γ	Maximum number of storage systems allowed.
γ	Budget of capital investment cost for storage systems (\$).
η	Annual discount rate of ESS investment.

Cost Coefficients

C_m^H	Energy rating cost of storage devices located at bus m (\$/MWh).
C_m^R	Power rating cost of storage devices located at bus m (\$/MW).
C_m^F	Fixed operation and maintenance cost of storage devices located at bus m (\$/MW/day).
C_m^V	Variable operation and maintenance cost of storage devices located at bus m (\$/MWh).
V_m^L	Value of load loss (VOLL) at bus m (\$/MWh).
U_n^G	Fixed generation cost of conventional unit n (\$).
V_n^G	Variable generation cost of conventional unit n (\$/MWh).

First-Stage Decision Variables

a_m	Binary variable indicating if ESS is placed at bus m.
h_m	Energy rating of storage system at bus m (MWh).
r_m	Power rating of storage system at bus m (MW).

Second-Stage Decision Variables

g_{ntd}^s	Generation output of generator n during time step t day d, in scenario s (MW).

Manuscript received December 16, 2014; revised April 15, 2015 and August 11, 2015; accepted August 25, 2015. Date of publication November 03, 2015; date of current version December 11, 2015. Paper no. TSTE-00709-2014.

The authors are with the Department of Electrical and Computer Engineering, Texas A&M University, College Station, TX 77843 USA (e-mail: xiongpengnus@gmail.com; singh@ece.tamu.edu).

Digital Object Identifier 10.1109/TSTE.2015.2482939

l^s_{mtd} Load loss at bus m during time step t day d, in scenario s (MW).
p^s_{mtd} Discharging power of storage unit at bus m during time step t day d, in scenario s (MW).
q^s_{mtd} Charging power of storage unit at bus m during time step t day d, in scenario s (MW).
s^s_{mtd} Energy state of charge of storage unit at bus m during time step t day d, in scenario s (MWh).
v^s_{ntd} Generation cost of conventional unit n during time step t day d, in scenario s (\$).
w^s_{td} Wind power output during time step t day d, in scenario s (MW).

Others

$\mathbb{N}(s,t)$ Node of the scenario tree, during time step t, scenario s.
P^s_d Probability of the wind power realization in day d, in scenario s.
W^s_{td} Wind power realization during time step t day d, in scenario s (MW).
δ The average daily operating cost (\$).
$|\mathcal{D}|$ Number of elements in set $\mathcal{D}$.

I. Introduction

WIND ENERGY industry has seen a cumulative growth rate of around 26% for the past eighteen years. The total wind power capacity is expected to reach nearly 2000 GW by 2030 in an advanced scenario, and to supply between 16.7% and 18.8% of global electricity demand [1]. Although wind energy is sustainable and emission-free, it is largely intermittent and subject to a high level of uncertainty. The forecast error of wind can be over 10% [2]–[4], so it is still difficult to efficiently integrate wind power with high penetration.

The ESS is considered a promising technology for mitigating the volatility of renewable energy generation and for better load management. Previous studies have shown that ESS can help mitigate wind power uncertain fluctuations [5], and enhance system operation in both economic and reliability perspectives [6]–[10]. However, since this technology is still expensive, the scale of ESS, in terms of energy and power ratings, should be optimally sized in order to better justify its economic viability. ESS sizing problems can be solved by stochastic programming approaches [9]–[11], or by sensitivity analysis based on simulation techniques [12].

Besides the size, the location of ESS in a power system is no less important, because system operation and wind integration may be greatly affected by transmission congestions [13]. Given fixed ESS sizes, the optimal location of storage units can be determined by a two-stage robust optimization formulation presented in [14]. This approach minimizes the worst-case total cost over a selected scenario set, so there is no need to make strong assumptions on the distribution of uncertain parameters. Several studies have also been proposed to optimize the location and size of ESS at the same time. Ref. [6], for instance, applies a genetic algorithm to solve the ESS planning optimization problem, where the efficiency of wind power utilization is maximized. An optimal planning scheme of ESS, based on the assumption that the operation of storage devices follows some predefined cycles, is discussed in [15], for minimizing the yearly cost of ESS construction and system operation.

For most previous studies that apply a stochastic optimization framework to solve the optimal planning of ESS, perfect information on system uncertainties in the second-stage operation problem is assumed. In the intraday operation practice, however, uncertain factors, such as the volatile wind power generation, cannot be forecasted accurately for the entire time horizon. The uncertainty of wind power is realized gradually, and part of the operating decisions must be determined in a *here-and-now* manner, i.e., before the future outcomes of wind power are observed. The remaining *wait-and-see* decisions can be made, as the outcomes of wind power are revealed in succession. This *nonanticipative* decision-making procedure [16] should be properly modeled, in order to reflect how system recourse actions under uncertainty are affected by intertemporal operating constraints, such as the ramp-rate limits of generators, and the ESS state of charge transition.

One of the main contributions of this paper is that a two-stage stochastic ESS planning model for determining both optimal locations and optimal sizes of ESS under uncertain wind power is proposed. The ESS planning decisions are made in the first-stage problem, before the observation of future wind power outcomes, and a daily operation model is considered in the second stage to assess the influence of ESS installation. Second, unlike the prior studies on ESS planning [9]–[11] that assume perfect information in the operation stage, a quantile-based scenario tree model [17] is applied here to address the nonanticipative process of decision-making in the second-stage daily operations. This scenario tree structure is constructed based on the autocorrelation of time series forecast errors, so the uncertainty of wind power generation can be well captured. Finally, in order to address computational difficulties, a Benders decomposition algorithm is used to solve this ESS optimization model in a timely manner. Previous research works on power system planning [18]–[20] have shown that this method should be more effective in attaining better optimality than genetic-inspired solutions [6], [7].

In Section II, the ESS planning formulation is discussed in detail, and the Benders decomposition algorithm used to solve this formulation is presented in Section III. Case studies are provided in Section IV to demonstrate the influence of ESS on power system operation, and to analysis the tradeoff between ESS investment and operating cost. Section V concludes our work.

II. Problem Formulation

A. Storage Planning Model

In the storage planning model, we consider a binary variable a_m that equals to one if an ESS is installed at bus m and zero otherwise. Let continuous variables h_m and r_m represent the

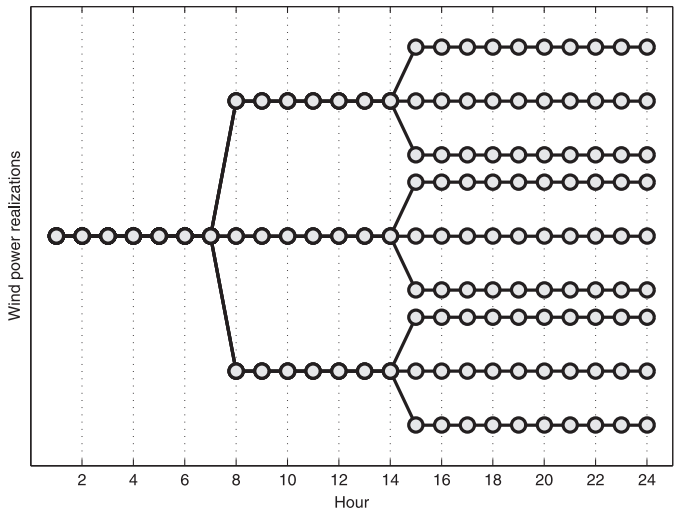

Fig. 1. Nine-realization example of scenario tree.

energy rating and power rating of storage units, respectively. These decision variables are subject to constraints (1)–(3)

$$\sum_{m\in\mathcal{M}} a_m \le \Gamma \tag{1}$$

$$H_m^{\min} a_m \le h_m \le H_m^{\max} a_m \quad \forall m \in \mathcal{M} \tag{2}$$

$$R_m^{\min} a_m \le r_m \le R_m^{\max} a_m \quad \forall m \in \mathcal{M}. \tag{3}$$

Inequality (1) suggests that the total number of storage systems constructed should be no more than Γ. The size of each ESS, in terms of the energy rating and power rating, is constrained by (2) and (3).

B. Scenario Tree for Wind Power Generation

A scenario tree model similar to [8] is applied to approximate the stochastic nature of wind power generation. This technique is suitable for modeling recourse actions of generators and storage units as system uncertainties are realized in succession. Such a scenario tree is constructed by considering several periods, and each period covers a number of hours. It is assumed that the outcome of wind power for a period is realized at the beginning of this period. The uncertainty of wind power for each period is represented by some discrete branches, thus a tree-shaped structure.

Fig. 1 shows an example of a scenario tree consisting three periods for the 24-h operation horizon. Each node of the scenario tree represents a wind power outcome associated with a probability for the corresponding time step. Following the quantile-based scenario tree technique in [17], wind outcome values and the associated probabilities can be calculated by exploiting the autocorrelated forecast errors from time series models. Decisions for all root nodes are, here-and-now, determined before the observation of uncertain wind power in the future, so they are required to be identical among all scenarios sharing the same root. Recourse decisions can then be made for subsequent branch nodes, after the outcome of wind power in each scenario is observed.

C. Daily Operation Model

In order to evaluate the effects of ESS on system operation, a daily operation model is considered in the proposed formulation. The decision variables of this operation model are subject to generator, storage, and system-wide constraints, shown below.

1) Generator Constraints: The power output of conventional thermal units is constrained by the generation capacity and ramp-rate limitations, expressed by (4)–(6)

$$G_n^{\min} \le g_{ntd}^s \le G_n^{\max} \quad \forall n \in \mathcal{N}, t \in \mathcal{T}, d \in \mathcal{D}, s \in \mathcal{S} \tag{4}$$

$$g_{n(t+1)d}^s - g_{ntd}^s \le R_n^R \quad \forall n \in \mathcal{N}, t \in \mathcal{T}, d \in \mathcal{D}, s \in \mathcal{S} \tag{5}$$

$$g_{ntd}^s - g_{n(t+1)d}^s \le R_n^R \quad \forall n \in \mathcal{N}, t \in \mathcal{T}, d \in \mathcal{D}, s \in \mathcal{S}. \tag{6}$$

2) Generation Cost: The generation cost of conventional units, denoted by v_{ntd}^s, is expressed as a linear function (7)

$$v_{ntd}^s = V_n^G g_{ntd}^s + U_n^G \quad \forall n \in \mathcal{N}, t \in \mathcal{T}, d \in \mathcal{D}, s \in \mathcal{S}. \tag{7}$$

3) Wind Power Generation: The generation of wind energy source, denoted by w_{td}^s, should be below the available wind power W_{td}^s, expressed as constraints (8)

$$0 \le w_{td}^s \le W_{td}^s, \quad t \in \mathcal{T}, d \in \mathcal{D}, s \in \mathcal{S}. \tag{8}$$

4) Storage Constraints: The decision variables of ESS are subject to constraints below

$$0 \le p_{mtd}^s \le r_m \quad \forall m \in \mathcal{M}, t \in \mathcal{T}, d \in \mathcal{D}, s \in \mathcal{S} \tag{9}$$

$$0 \le q_{mtd}^s \le r_m \quad \forall m \in \mathcal{M}, t \in \mathcal{T}, d \in \mathcal{D}, s \in \mathcal{S} \tag{10}$$

$$0 \le s_{mtd}^s \le h_m \quad \forall m \in \mathcal{M}, t \in \mathcal{T}, d \in \mathcal{D}, s \in \mathcal{S} \tag{11}$$

$$s_{m(t+1)d}^s = s_{mtd}^s - \frac{1}{\alpha_m^D} p_{mtd}^s + \alpha_m^C q_{mtd}^s \quad \forall m \in \mathcal{M}, t \in \mathcal{T}, d \in \mathcal{D}, s \in \mathcal{S}. \tag{12}$$

Inequalities (9) and (10) restrict the discharging/charging power below the power rating of ESS, and the energy capacity constraints are imposed by (11). The energy transition in ESS is expressed by (12).

5) Power Flow: The power balance and transmission capacity constraints are expressed by (13) and inequality (14), respectively,

$$\sum_{n\in\mathcal{N}} g_{ntd}^s + \sum_{m\in\mathcal{M}} (p_{mtd}^s - q_{mtd}^s) + w_{td}^s = \sum_{m\in\mathcal{M}} (D_{mtd} - l_{mtd}^s) \quad \forall t \in \mathcal{T}, d \in \mathcal{D}, s \in \mathcal{S} \tag{13}$$

$$-F_l \le K_{wl} w_{td}^s + \sum_{m\in\mathcal{M}} \sum_{n\in\mathcal{N}_m} K_{ml} g_{ntd}^s + \sum_{m\in\mathcal{M}} K_{ml} (p_{mtd}^s - q_{mtd}^s) - \sum_{m\in\mathcal{M}} K_{ml} (D_{mtd} - l_{mtd}^s) \le F_l \quad \forall l \in \mathcal{L}, t \in \mathcal{T}, d \in \mathcal{D}, s \in \mathcal{S}. \tag{14}$$

A dc power flow model [21] is used in (14) to the transmission network. This simplification is considered valid in many previous studies [6], [7], [12], [14], because ESS mainly affects

the supply and consumption of real power, while the impact on reactive power is less significant. The influence of ESS on power transmission systems can be captured by expression (14), which affects the selection of the optimal ESS locations.

6) Nonanticipativity Constraints: For power systems installed with wind energy, some decisions must be determined before the observation of future wind power outcomes, and these decisions, especially the charge state of ESS, may greatly affect the following system operations. As a result, it is more appropriate to apply a nonantivipative decision-making timeline in the operation model, rather than the perfect information assumption.

The nonanticipativity constraints force decisions for various scenarios made before the realization of uncertainty to be identical. Let $\mathbb{N}(t,s)$ denote the node of the selected scenario tree at time step t in scenario s, and let $\mathbf{y}_{td}^{s}$ be the vector containing all operating decision variables in day d for the corresponding node, i.e., $\mathbf{y}_{td}^{s}=(g_{ntd}^{s},w_{ktd}^{s},p_{mtd}^{s},q_{mtd}^{s},s_{mtd}^{s},l_{mtd}^{s})$. Nonanticipativity constraints in the following form are included in the operation model, so that decisions for the root nodes are nonanticipative

$$\mathbf{y}_{td}^{s}=\mathbf{y}_{td}^{s'},\quad \text{if } \mathbb{N}(s,t)=\mathbb{N}(s',t) \quad \forall t\in\mathcal{T},\forall d\in\mathcal{D},\forall s,s'\in\mathcal{S}. \tag{15}$$

D. Objective Function and the Budget Constraint

Previous literatures [9], [10], [14], [15] attempt to minimize the total expense of ESS capital cost and system operating cost. In this paper, we try to minimize the average daily operating cost, while the capital cost is subject to some budget constraints. The advantage of this formulation is that besides a single solution corresponding to the optimal total cost, an entire cost frontier that indicating the tradeoff between ESS capital cost and daily operating cost can be achieved.

Based on the daily operation model discussed in the prior subsection, the operating cost for a day d, in scenario s, can be expressed as follows:

$$z_{d}^{s}=\sum_{m\in\mathcal{M}}C_{m}^{F}r_{m}+\sum_{t\in\mathcal{T}}\sum_{m\in\mathcal{M}}C_{m}^{V}p_{mtd}^{s} +\sum_{t\in\mathcal{T}}\sum_{n\in\mathcal{N}}v_{ntd}^{s}+\sum_{t\in\mathcal{T}}\sum_{m\in\mathcal{M}}V_{m}^{L}l_{mtd}^{s}\quad\forall d\in\mathcal{D},s\in\mathcal{S} \tag{16}$$

where the first and second terms are, respectively, the daily fixed and variable operations/maintenance (O&M) cost of ESS. The third term is the generation cost, and the last term penalizes load curtailment l_{mtd}^{s} by a high VOLL, denoted by V_{m}^{L}.

This formulation considers the expected operating cost over all wind power realizations in each day. In order to account for various load and wind power profiles in a long run, the objective is to minimize the average daily operating cost for some representative days, expressed by (17), where the objective value is denoted by δ

$$\delta=\min\frac{1}{|\mathcal{D}|}\sum_{d\in\mathcal{D}}\sum_{s\in\mathcal{S}}P_{d}^{s}z_{d}^{s}. \tag{17}$$

The total capital cost of ESS is constrained below a budget of capital cost investment, denoted by γ

$$\sum_{m\in\mathcal{M}}\left(C_{m}^{H}h_{m}+C_{m}^{R}r_{m}\right)\leq\gamma. \tag{18}$$

The constant C_{m}^{H} is the capital cost of energy rating, and C_{m}^{R} is the cost of power rating.

E. Compact Matrix Form

This section expresses the ESS planning problem as a compact matrix form, in order to better present the decomposition algorithm. All first-stage variables, including ESS planning decisions a_m, h_m, and r_m, are denoted by x. Note that the placement indicator a_m is binary, and according to [16], such integrality restrictions in the first stage does not change the properties of the recourse problem, so they can be treated the same as the continuous case in the solution procedure. The vector of operating decisions for all scenarios in each day d is denoted by $\mathbf{y}_d$, and the two-stage optimization problem presented above can be expressed as the following compact matrix form:

$$\min\quad c^{T}x+\frac{1}{|\mathcal{D}|}\sum_{d\in\mathcal{D}}q^{T}y_{d} \tag{19}$$

$$\text{s.t. } Ax\leq b \tag{20}$$

$$Cx+Hy_{d}\leq\mathbf{h}_{d}\quad\forall d\in\mathcal{D} \tag{21}$$

$$Ux+Vy_{d}=\mathbf{v}_{d}\quad\forall d\in\mathcal{D} \tag{22}$$

$$x\geq 0,\mathbf{y}_{d}\geq 0\quad\forall d\in\mathcal{D}. \tag{23}$$

The objective function (17) is expressed as the vector form (19), where all first terms of (16) that contain first-stage decision variables are expressed as $c^{T}x$, and the remaining terms are expressed by the linear function of second-stage decision variables $\mathbf{y}_d$. Constraints (1)–(3), as well as constraints (18), are included in constraints (20). Expression (21) represents all inequality constraints in the operating problem, namely, generator constraints (4)–(6), wind power constraints (8), storage limitations (9)–(11), and transmission capacity constraints (14). Equality constraints (7), (12), and (13), together with all nonanticipativity constraints (15), are represented by (22). Coefficients of constraints (21) and (22) are the same for each day d, except that the right-hand-side vector $\mathbf{h}_d$ and $\mathbf{v}_d$ may take different values. All decision variables should be nonnegative, as indicated by (23).

It is observed that the operation model for each day d is independent, so a Benders decomposition algorithm can be used to solve this optimization problem in an efficient manner. Details of this algorithm are given in the next section.

III. Solution Method

The dimension of the proposed formulation is huge, because the operation model considers many days with various wind power realizations. As a result, this optimization problem is difficult to be solved directly. A multicut Benders decomposition

algorithm is, therefore, presented in this section to provide an efficient solution.

The overall problem (19)–(23) is reformulated into the equivalent form (24), in order to facilitate the discussion on the algorithm

$$\begin{aligned} Z^o = \min\ & \boldsymbol{c}^T\boldsymbol{x} + \frac{1}{|\mathcal{D}|}\sum_{d\in\mathcal{D}}\theta_d \\ \text{s.t. } & \theta_d \geq \boldsymbol{q}^T\boldsymbol{y}_d \quad \forall d\in\mathcal{D} \\ & \boldsymbol{A}\boldsymbol{x} \leq \boldsymbol{b} \\ & \boldsymbol{C}\boldsymbol{x} + \boldsymbol{H}\boldsymbol{y}_d \leq \mathbf{h}_d \quad \forall d\in\mathcal{D} \\ & \boldsymbol{U}\boldsymbol{x}_d + \boldsymbol{V}\boldsymbol{y}_d = \mathbf{v}_d \quad \forall d\in\mathcal{D} \\ & \boldsymbol{x}\geq 0, \boldsymbol{y}_d \geq 0 \quad \forall d\in\mathcal{D}. \end{aligned} \tag{24}$$

The objective value of problem (24) is denoted by Z^o. This formulation suggests a two-stage decision-making procedure. In this formulation, the ESS planning decisions x are determined in the first stage without knowing the daily load and wind profile. The operating decisions are made according to the observation of various load patterns and wind uncertainties, once the planning decisions x are fixed.

A. Relaxed Subproblems

It is observed that Benders decomposition may not be able to provide a tight lower bound, so an extra lower bound is generated to improve convergence by solving a series of subproblems given below

$$\begin{aligned} Z_d^{\mathrm{RS}} = \min\ & \boldsymbol{c}^T\boldsymbol{x}_d + q^T\boldsymbol{y}_d \\ \text{s.t. } & \boldsymbol{A}\boldsymbol{x}_d \leq \boldsymbol{b} \\ & \boldsymbol{C}\boldsymbol{x}_d + \boldsymbol{H}\boldsymbol{y}_d \leq \mathbf{h}_d \\ & \boldsymbol{U}\boldsymbol{x}_d + \boldsymbol{V}\boldsymbol{y}_d = \mathbf{v}_d \\ & \boldsymbol{x}_d \geq 0, \boldsymbol{y}_d \geq 0. \end{aligned} \tag{25}$$

Compared with problem (24), these subproblems are relaxed and can be decoupled and solved independently, because the ESS planning decisions x_d are not required to be identical for all days $d\in\mathcal{D}$. The average value of the optimal objective Z_d^{RS} overall all days is a lower bound of the two-stage problem (24); hence, the lower bound constraint (26)

$$\boldsymbol{c}^T\boldsymbol{x} + \frac{1}{|\mathcal{D}|}\sum_{d\in\mathcal{D}}\theta_d \geq Z^o \geq \frac{1}{|\mathcal{D}|}\sum_{d\in\mathcal{D}} Z_d^{\mathrm{RS}}. \tag{26}$$

B. Benders Subproblems

Let $\hat{x}^i$ be a given planning decision in the ith iteration, the operation problem for each day is expressed as Benders subproblem (27)

$$\begin{aligned} Z_d^{\mathrm{BDS}}(i) = \min\ & \boldsymbol{q}^T\boldsymbol{y}_d \\ \text{s.t. } & \boldsymbol{H}\boldsymbol{y}_d \leq \mathbf{h}_d - C\hat{\boldsymbol{x}}^i \\ & \boldsymbol{V}\boldsymbol{y}_d = \mathbf{v}_d - U\hat{\boldsymbol{x}}^i \\ & \boldsymbol{y}_d \geq 0. \end{aligned} \tag{27}$$

This problem is solved as the dual form (28)

$$\begin{aligned} Z_d^{\mathrm{BDS}}(i) = \max\ & \left(\mathbf{h}_d - \boldsymbol{C}\hat{\boldsymbol{x}}^i\right)^T\boldsymbol{\lambda}_d + \left(\mathbf{v}_d - \boldsymbol{U}\hat{\boldsymbol{x}}^i\right)^T\boldsymbol{\mu}_d \\ \text{s.t. } & \boldsymbol{H}^T\boldsymbol{\lambda}_d + \boldsymbol{V}^T\boldsymbol{\mu}_d \leq q \\ & \boldsymbol{\lambda}_d \leq 0 \end{aligned} \tag{28}$$

where λ_d and μ_d are the dual variables, respectively, associated with the inequality and equality constraints in (27).

By solving the dual problem (28), an upper bound $Z^U(i)$ of problem (24), given below, can be derived based on the optimal objective Z_d^{BDS}

$$Z^U(i) = \boldsymbol{c}^T\hat{\boldsymbol{x}}^i + \frac{1}{|\mathcal{D}|}\sum_{d\in\mathcal{D}} Z_s^{\mathrm{BDS}}(i) \geq Z^o. \tag{29}$$

Let $(\hat{\lambda}_d^i, \hat{\mu}_d^i)$ denote the optimal solution to the dual problem (28) in the ith iteration, the Benders cuts are given as constraints (30)

$$\begin{aligned} \theta_d \geq & -(\hat{\boldsymbol{\lambda}}_d^i)^T\boldsymbol{C}\boldsymbol{x} - (\hat{\boldsymbol{\mu}}_d^i)^T\boldsymbol{U}\boldsymbol{x} \\ & +(\hat{\boldsymbol{\lambda}}_d^i)^T\boldsymbol{h}_d + (\hat{\boldsymbol{\mu}}_d^i)^T\boldsymbol{v}_d \quad \forall d\in\mathcal{D}. \end{aligned} \tag{30}$$

C. Master Problem

By including the lower bound constraint (26) and the Benders cuts (30) in prior iterations, the master problem in the Ith iteration can be constructed as follows:

$$\begin{aligned} Z^M(I) = \min\ & \boldsymbol{c}^T\boldsymbol{x} + \frac{1}{|\mathcal{D}|}\sum_{d\in\mathcal{D}}\theta_d \\ \text{s.t. } & \boldsymbol{A}\boldsymbol{x} \leq \boldsymbol{b} \\ & \boldsymbol{x} \geq 0 \\ & \boldsymbol{c}^T\boldsymbol{x} + \frac{1}{|\mathcal{D}|}\sum_{d\in\mathcal{D}}\theta_d \geq \sum_{d\in\mathcal{D}} Z_d^{\mathrm{RS}} \\ & \theta_d \geq -(\hat{\boldsymbol{\lambda}}_d^i)^T\boldsymbol{C}\boldsymbol{x} - (\hat{\boldsymbol{\mu}}_d^i)^T\boldsymbol{U}\boldsymbol{x} \\ & \quad + (\hat{\boldsymbol{\lambda}}_d^i)^T\boldsymbol{h}_d + (\hat{\boldsymbol{\mu}}_d^i)^T\boldsymbol{v}_d \quad \forall d\in\mathcal{D} \\ & \quad \forall i = 1,2,\ldots,I. \end{aligned} \tag{31}$$

The optimal solution is used as the first-stage decision in the next iteration, thus denoted by $\hat{x}^{I+1}$. The objective value $Z^M(I)$ is used to update the lower bound of this algorithm.

D. Algorithm Steps

The Benders decomposition algorithm presented in this section is different from the conventional version [16], in that a lower bound constraint (26) is applied to improve the convergence. Besides, for all feasible ESS planning decisions x, the daily operation problem should always be feasible, because load curtailment or wind power spillage may occur in adverse scenarios to prevent infeasibility. Hence, there is no need to generate feasibility cuts for this two-stage problem.

Let ϵ be the tolerance of the relative dual gap, the specific steps of this algorithm are listed as follows.

Step 0) Set iteration count $I = 1$. Let $\hat{\boldsymbol{x}}^1 = 0$ and $\hat{\boldsymbol{x}}^{\mathrm{opt}} = 0$. The upper bound $\mathrm{UB} = +\infty$ and lower bound $\mathrm{LB} = 0$.

TABLE I
FUEL COST OF GENERATION

Fuel type	Cost ($/MMBTU)
No.6 oil	10.82
No.2 oil	15.39
Coal	2.26
Nuclear	0.6

TABLE II
ESS DATA

Limits	Max. capacity	1500 MWh
	Min. capacity	100 MWh
	Max power rate	350 MW
	Min power rate	35 MW
Capital cost	Capacity cost	3000 $/MWh
	Power cost	560 000 $/MW
O&M cost	Fixed O&M cost	1200 $/MWh/year
	Variable O&M cost	1.5 $/MWh
Efficiency	Charge	90.0%
	Discharge	87.5%

Step 1) Solve the relaxed subproblem (25) over all days $d \in \mathcal{D}$ to obtain the lower bound constraint (26).

Step 2) For the given $\hat{\boldsymbol{x}}^I$, solve subproblems (28) for all days $d \in \mathcal{D}$ to obtain $Z^U(I)$ and Benders cuts (30). Set $\hat{\boldsymbol{x}}^{\text{opt}} = \hat{x}^I$ if $\text{UB} > Z^U(I)$. Update UB as $\text{UB} = \min\left\{Z^U(I), \text{UB}\right\}$.

Step 3) Append the Benders cut constraints (30) to the master problem (31). Solve the master problem to obtain $\hat{\boldsymbol{x}}^{I+1}$. Update the lower bound $\text{LB} = Z^M(I)$.

Step 4) Check convergence. If the relative dual gap is not larger than the tolerance ϵ, i.e., $(\text{UB} - \text{LB})/\text{LB} \leq \epsilon$, or if the maximum number of iterations is reached, terminate the program and return $\hat{\boldsymbol{x}}^{\text{opt}}$ as the optimal solution, otherwise set iteration count $I = I + 1$ and go back to Step 2).

IV. CASE STUDIES

The proposed approach is applied to one area of the modified IEEE RTS-96 [22], consisting of 24 buses and 32 generators. The fuel cost of generation [23] is provided in Table I, and the VOLL is assumed to be 2000$/MWh. Because the daily load patterns in one season are unlikely to vary too much, we consider 28 days (one week for each season) in the daily operation model. In order to highlight the influence of locations on ESS planning, capacities of all transmission lines are reduced by 20%. The parameters of ESS, based on the compressed air energy storage (CAES) case in [24], are listed in Table II.

It is assumed that a wind farm with a capacity of 400 MW is placed at bus 13. Due to the extra generation capacity of wind power, the original system may be too reliable to reveal any risks of congestion or load loss, so the electricity demand is increased by 35% to create a less reliable case. The uncertain output of wind power generation is represented by the nine-realization scenario tree depicted by Fig. 1. Such a scenario tree has three branches, defined to be the 0.05, 0.5, and 0.95 quantile of the distribution of forecast errors. The wind power outcome and the associated probability of each node can then be calculated according to the quantile-based scenario tree technique in [17]. In this paper, it is assumed that the forecast error of wind power generation follows a second-order autoregressive model [17], [25]. Parameters of this autoregressive model, together with other seasonal and diurnal constants of wind power generation, can be found in [25].

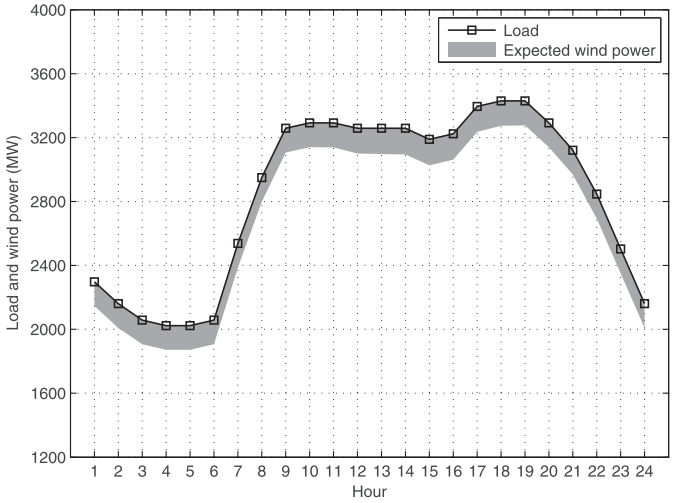

Fig. 2. Load and expected wind power for a winter weekday.

In this section, we will first compare the results of cases with and without storage units, for demonstrating the influence of ESS on power systems integrated with wind power generation. A cost frontier is then calculated to analyze the tradeoff between the capital cost of ESS and the daily operating expenses. Finally, the computational experience of the proposed method is discussed.

A. ESS in System Operation

In this section, we consider a case with the budget of ESS capital cost not exceeding 80 million dollars. The solution of the planning problem suggests that the optimal location of ESS is bus 15, and the energy rating and power rating of the storage unit should be 867.4 MWh and 138.2 MW, respectively.

Fig. 2 shows the load and expected wind power for a winter weekday, and Fig. 3 displays the corresponding charging states of storage devices under wind uncertainty. Operating decisions are made based on the scenario tree model shown by Fig. 1. Decisions for the first few hours should be determined before the uncertainty of wind power generation is fully realized, so they must be identical for all scenarios. As the actual wind power output is gradually revealed in latter periods, recourse decisions can be made to achieve the lowest cost under every realization of wind. It can be seen that the nonanticipative decision-making process in daily system operation is well captured by this scenario tree model.

It is also observed that ESS in this case mainly charges during the first 7 h, when the load is lower than the rest of the day. The storage system works mostly in discharging mode after 9 A.M., as the electrical load approaches its peak value. This figure suggests that ESS is capable of shifting load from peak hours to off-peak hours.

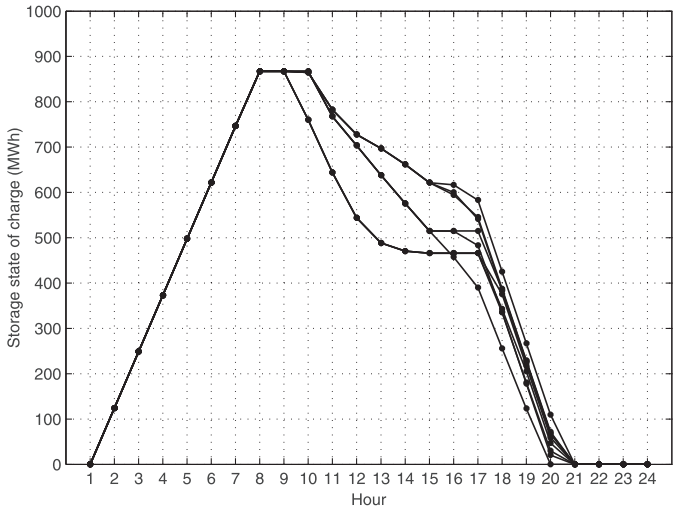

Fig. 3. Storage state of charge under different wind power realizations for a winter weekday, when the ESS budget of investment is 80 million dollars.

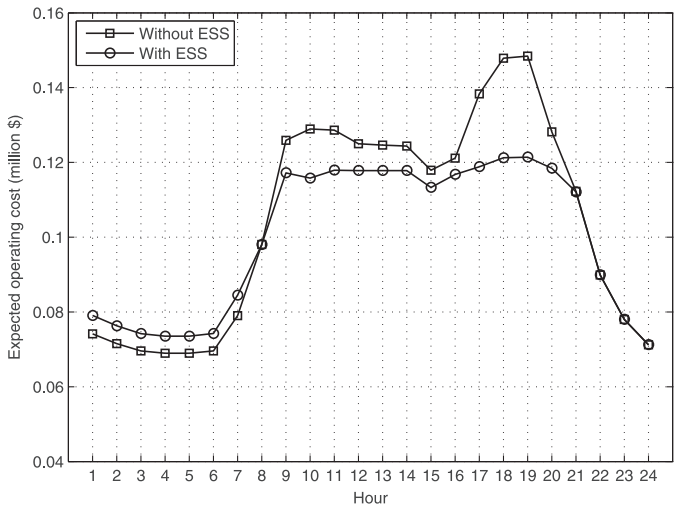

Fig. 4. Expected hourly operating cost for a winter weekday, when the ESS budget of investment is 80 million dollars.

As a result, before ESS is added to the test system, the average daily operating cost is found to be 1946105.69$, and load curtailment may occur at bus 15 when the wind power generation is much lower than predicted. After the installation of ESS, there is no load curtailment in all selected scenarios. Due to load-shifting capability of ESS, the average daily operating cost drops to 1906397.89$, much lower than the case without ESS. The reduction of operating expenses can be better demonstrated in Fig. 4, which shows the expected hourly operating cost over all nine scenarios for the same winter weekday. It is observed that in the first 7 h, when the demand is low, the operating cost of the case with ESS is higher than the case without ESS, suggesting that extra power is generated to charge the storage unit. The operating cost increases greatly during peak hours between 9 A.M. and 21 P.M. For the ESS case, instead of relying on expensive peaking power generators, the energy stored in previous hours can be used to supply the demand, so the operating cost during this period is much lower than the case without ESS. If the budget of ESS investment is increased to promote

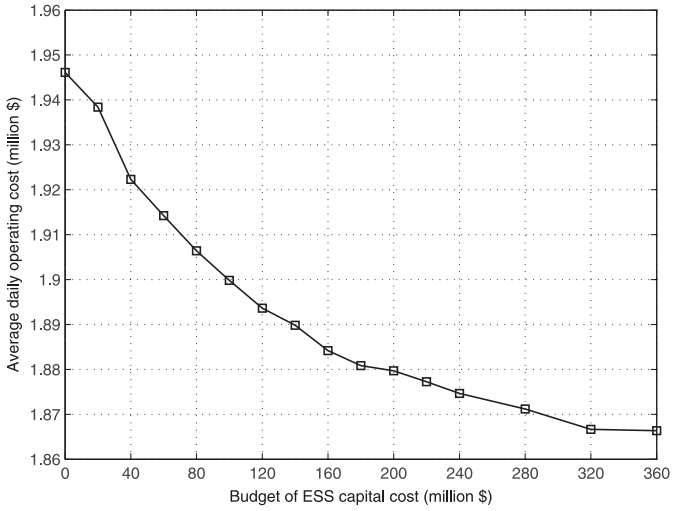

Fig. 5. Capital/operating cost frontier of ESS.

the scale of storage units, we may be able to shift larger amount of peak-hour load, thus further reducing the operating cost. This point is supported by the discussion in the next section.

B. Tradeoff Between ESS Investment and Operating Cost

The tradeoff between the capital investment on ESS and the daily operating cost is shown by a capital/operating cost frontier, shown by Fig. 5. This frontier is attained by solving planning problems with budget increasing from zero to 360 million dollars.

The daily operating cost is the highest when no ESS is constructed in the test system. As the budget rises, the operating cost decreases steadily, mainly due to the increasing load shifting capability of ESS. It is observed that this cost curve becomes "flat" when the budget is quite high, implying that the reduction of daily operating cost is diminishing as the investment on ESS rises.

The best tradeoff between the capital investment on ESS and the operating cost can be determined according to the overall daily expense of power system throughout the lifespan of storage devices, expressed below

$$\delta + \frac{1}{365}\frac{\eta(1+\eta)^{\mathrm{NS}}}{(1+\eta)^{\mathrm{NS}}-1}\cdot\gamma. \tag{32}$$

The first term δ indicates the average daily operating cost, and the second term is the capital cost of ESS normalized on a daily basis according to the annuity model [26], where NS is the lifespan of storage units in number of years, and η is the discount rate of investment in terms of annual interest. The most efficient investment budget can be calculated by searching for the minimum value of expression (32) among all solutions. For example, suppose that the discount rate $\eta = 4\%$ per year, the best scale of ESS investment against the lifespan of storage devices is shown in Fig. 6.

The case studies suggest that the investment on ESS should be increased if technological advances extend the lifespan of energy storage devices. It can also be seen that the scale of investment should not exceed 180 million dollars, even if

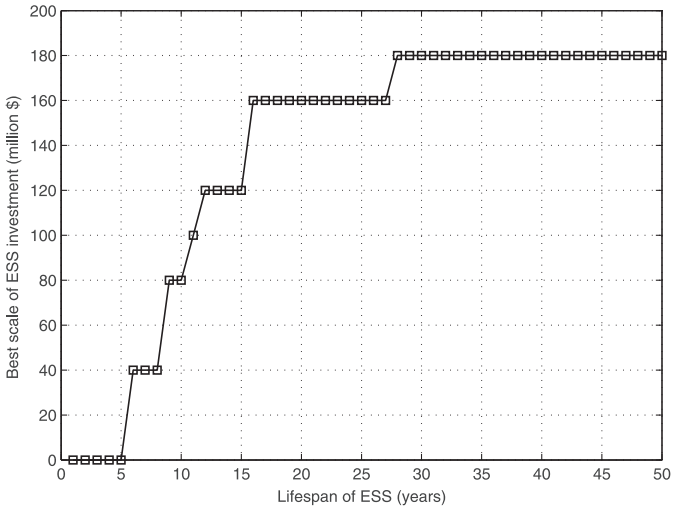

Fig. 6. Best scale of ESS investment.

the lifespan of storage units is as long as 50 years. This is because as the budget of ESS investment is over 180 million dollars, the improvement in daily operation efficiency is very trivial. The comparison between the 180-million-budget case and the 360-million-budget case shows that the reduction of operating cost is merely 0.76%, although the budget of investment is doubled. In fact, even if there is no budget limitation imposed (infinite budget), the average daily operating cost is 1860510.02$, only about 1% lower than the case with a 180 million dollar budget.

Two reasons may contribute to the fact that the reduction of daily operating cost becomes insignificant as the ESS investment further increases: 1) enlarging ESS scale also rises the O&M cost; and 2) the load shifting capability of ESS might be weakened by the transmission limitations. This is why the location of storage units is as important as the scales. The optimal locations, as well as the optimal scale of ESS under various budget constraints, are given in Table III.

It is observed that storage devices should be placed around the location that is likely to have power deficiency, which is bus 15 in this case. When the budget is low, the most efficient way of planning is concentrating all available resources to build ESS at bus 15. The only exception is the case with a budget of 100 million dollars, ESS is installed at bus 15 as well as bus 24, which is directly connected to bus 15 through a 400-MW transmission line. When the budget is between 140 and 280 million dollars, ESS is likely to be built at two locations. The optimal combination should be bus 3 or bus 15, together with bus 24. As the budget is over 320 million dollars, the investment is sufficient to build ESS at three or even four different locations. However, Fig. 5 shows that the improvement of operation efficiency caused by the extra storage unit is almost negligible.

C. Computational Experience

In this paper, all ESS planning problems are solved by CPLEX 12.6.2 on a mobile workstation with a 2.20GHz quad-core Intel i7 processor and 4GB memory. It is found that the problem dimension is so large that there is an out of memory error when these problems are solved directly. As the Benders decomposition algorithm is applied to solve these planning problem, the tolerance of the relative dual gap is set to be $\epsilon = 2 \times 10^{-3}$, and the MIP gaps of both the relaxed subproblems (25) and the master problem (31) are also set to be $10^{-}3$. The solution time of each case is shown in Table IV. The average computation time for all cases is around 9 min. The longest solution time is about 24 min, as the budget of ESS investment is set to be 280 million dollars. It should be noted that in this decomposition algorithm, the time-consuming subproblems in

TABLE III
OPTIMAL LOCATION AND SIZE OF ESS

Budget (million $)	Location	Capacity (MWh)	Power rate (MW)
0	–	0	0
20	Bus 15	100.0	35.2
40	Bus 15	1091.9	65.6
60	Bus 15	666.8	98.8
80	Bus 15	867.4	138.2
100	Bus 15	1500.0	78.1
	Bus 24	1245.6	85.7
120	Bus 15	1500.0	196.4
140	Bus 15	673.9	115.0
	Bus 24	921.7	126.5
160	Bus 15	1032.7	135.6
	Bus 24	1034.9	139.0
180	Bus 15	1500.0	151.5
	Bus 24	1118.6	155.9
200	Bus 3	1500.0	168.2
	Bus 24	1213.8	174.4
220	Bus 3	1200.7	189.7
	Bus 24	1328.3	189.6
240	Bus 3	1393.6	209.8
	Bus 24	1415.1	203.7
280	Bus 15	1250.8	215.5
	Bus 24	1500.0	229.1
320	Bus 3	1500.0	165.0
	Bus 15	1500.0	221.2
	Bus 24	1497.4	161.2
360	Bus 2	1473.8	157.5
	Bus 5	1500.0	153.2
	Bus 9	1399.8	153.5
	Bus 15	1500.0	147.3

TABLE IV
SOLUTION TIME OF ESS PLANNING PROBLEMS

Budget (million $)	Solution time (min)
20	6.60
40	5.21
60	5.62
80	5.49
100	8.10
120	8.99
140	8.17
160	7.99
180	7.80
200	9.64
220	8.75
240	8.89
280	24.20
320	10.97
360	11.88

Step 1) and Step 2) are totally independent, which is well suited for the grid computing technology. The solution time is expected to be reduced greatly if these subproblems can be solved in parallel.

V. Conclusion

This paper addresses ESS planning problem for power systems integrated with uncertain wind power generation. The random forecast error of wind power is incorporated into the proposed formulation by a scenario tree model, where operating decisions are determined, as system uncertainties are gradually realized. Case studies conducted in this paper demonstrate an instance of a capital/operating cost curve. This curve can be applied to analyze the tradeoff between the capital cost of ESS and the daily system operating cost. The discussion on the tradeoff frontier also covers how the optimal planning decision of ESS, in terms of locations and sizes, evolves as the budget of capital investment increases. It is found in the numerical experiment that the proposed ESS planning problem cannot be solved directly. A Benders decomposition algorithm is, therefore, utilized to address the overall formulation by solving a sequence of much smaller master problems and subproblems. The experiment shows that this algorithm has decent computational efficiency. More research can be done in the future to further reduce the computational cost by applying the parallel computing technique.

References

[1] G. W. E. Council. (2014). *Global Wind Energy Outlook 2014* [Online]. Available: http://www.gwec.net/wp-content/uploads/2014/10/GWEO2014_WEB.pdf

[2] T. Solution and A. Scientific. (2003). *Overview of Wind Energy Generation Forecasting* [Online]. Available: http://www.uwig.org/forecst_overview_report_dec_2003.pdf

[3] H. Savage, J. Kennedy, B. Fox, and D. Flynn, "Managing variability of wind energy with heating load control," in *Proc. 43rd Int. Univ. Power Eng. Conf. (UPEC'08)*, Sep. 2008, pp. 1–5.

[4] B.-M. Hodge and M. Milligan. (2011). *Wind Power Forecasting Error Distributions Over Multiple Timescales* [Online]. Available: http://www.nrel.gov/docs/fy11osti/50614.pdf

[5] F. Luo, K. Meng, Z. Y. Dong, Y. Zheng, Y. Chen, and K. P. Wong, "Coordinated operational planning for wind farm with battery energy storage system," *IEEE Trans. Sustain. Energy*, vol. 6, no. 1, pp. 253–262, Jan. 2015.

[6] M. Ghofrani, A. Arabali, M. Etezadi-Amoli, and M. Fadali, "A framework for optimal placement of energy storage units within a power system with high wind penetration," *IEEE Trans. Sustain. Energy*, vol. 4, no. 2, pp. 434–442, Apr. 2013.

[7] M. Ghofrani, A. Arabali, M. Etezadi-Amoli, and M. Fadali, "Energy storage application for performance enhancement of wind integration," *IEEE Trans. Power Syst.*, vol. 28, no. 4, pp. 4803–4811, Nov. 2013.

[8] D. Swider, "Compressed air energy storage in an electricity system with significant wind power generation," *IEEE Trans. Energy Convers.*, vol. 22, no. 1, pp. 95–102, Mar. 2007.

[9] C. Abbey and G. Joós, "A stochastic optimization approach to rating of energy storage system in wind-diesel isolated grids," *IEEE Trans. Power. Syst.*, vol. 24, no. 1, pp. 418–426, Feb. 2009.

[10] S. Bahramirad, W. Reder, and A. Khodaei, "Reliability-constrained optimal sizing of energy storage system in a microgrid," *IEEE Trans. Power. Syst.*, vol. 3, no. 4, pp. 2056–2062, Dec. 2012.

[11] S. Dutta and R. Sharma, "Optimal storage sizing for integrating wind and load forecast uncertainties," in *Proc. IEEE PES Innov. Smart Grid Technol. (ISGT)*, Jan. 2012, pp. 1–7.

[12] N. Zhang *et al.*, "Planning pumped storage capacity for wind power integration," *IEEE Trans. Sustain. Energy*, vol. 4, no. 2, pp. 393–401, Apr. 2013.

[13] H. Holttinen *et al.*, "Impacts of large amounts of wind power on design and operation of power systems, results of IEA collaboration," *Wind Energy*, vol. 14, pp. 179–192, 2011.

[14] R. Jabr, I. Džafić, and B. Pal, "Robust optimization of storage investment on transmission networks," *IEEE Trans. Power. Syst.*, vol. 30, no. 1, pp. 531–539, Jan. 2015.

[15] H. Oh, "Optimal planning to include storage devices in power systems," *IEEE Trans. Power. Syst.*, vol. 26, no. 3, pp. 1118–1128, Aug. 2011.

[16] J. Birge and F. Louveaux, *Introduction to Stochastic Programming*. Berlin, Germany: Springer-Verlag, 1997.

[17] A. Sturt and G. Strbac, "Efficient stochastic scheduling for simulation of wind-integrated power systems," *IEEE Trans. Power. Syst.*, vol. 27, no. 1, pp. 323–334, Feb. 2012.

[18] P. Jirutitijaroen and C. Singh, "Stochastic programming approach for unit availability consideration in multi-area generation expansion planning," in *Proc. IEEE Power Eng. Soc. Gen. Meeting*, Jun. 2007, pp. 1–5.

[19] O. Tor, A. Guven, and M. Shahidehpour, "Congestion-driven transmission planning considering the impact of generator expansion," *IEEE Trans. Power Syst.*, vol. 23, no. 2, pp. 781–789, May 2008.

[20] Y. Gu, J. McCalley, and M. Ni, "Coordinating large-scale wind integration and transmission planning," *IEEE Trans. Sustain. Energy*, vol. 3, no. 4, pp. 652–659, Oct. 2012.

[21] S. Wang, D. Shahidehpour, D. Kirschen, S. Mokhtari, and D. Irisarri, "Short-term generation scheduling with transmission and environmental constraints using an augmented lagrangian relaxation," *IEEE Trans. Power. Syst.*, vol. 10, no. 3, pp. 1294–1301, Aug. 1995.

[22] Reliability Test System Task Force, "The IEEE reliability test system-1996," *IEEE Trans. Power. Syst.*, vol. 14, no. 3, pp. 1010–1020, Aug. 1999.

[23] U.S. Energy Information Administration. (2015, Jul.). *Short-Term Energy Outlook 2015* [Online]. Available: http://www.eia.gov/forecasts/steo/pdf/steo_full.pdf

[24] V. Viswanathan, M. Kintner-Meyer, P. Balducci, and C. Jin. (2013). National Assessment of Energy Storage for Grid Balancing and Arbitrage Phase II, Volume 2: Cost and Performance Characterization [Online]. Available: http://energyenvironment.pnnl.gov/pdf/National_Assessment_Storage_PHASE_II_vol_2_final.pdf

[25] A. Sturt and G. Strbac, "A times series model for the aggregate GB wind output circa 2030," in *Proc. IET Conf. Renew. Power Gener. (RPG'11)*, Sep. 2011, pp. 1–6.

[26] J. Schlabbach and K.-H. Rofalski, *Power System Engineering: Planning, Design, and Operation of Power Systems and Equipment*. Weinheim, Germany: Wiley-VCH, 2008.

Peng Xiong received the B.Eng. degree in electrical engineering from Zhejiang University, Hangzhou, China, in 2008, and the Ph.D. degree in electrical engineering from the National University of Singapore, Singapore, in 2013.

He is a currently a Postdoctoral Researcher with Texas A&M University, College Station, TX, USA. His research interests include the area of power system reliability and optimization.

Chanan Singh (S'71–M'72–SM'79–F'91) received the D.Sc. degree in electrical engineering from the University of Saskatchewan, Saskatoon, SK, Canada, in 1997.

He is currently a Regents Professor and Irma Runyon Chair Professor of Electrical and Computer Engineering with Texas A&M University, College Station, TX, USA. His research and consulting interests are the application of probabilistic methods to power systems.

Dr. Singh was the recipient of the 1998 Outstanding Power Engineering Educator Award given by the IEEE Power Engineering Society. In 2008, he was recognized with the Merit Award by the PMAPS International Society. In 2010, he was the inaugural recipient of the Roy Billinton Power System Reliability Award.